Mechanism of Suspension Polymerization of Uniform Monomer Droplets Prepared by Glass Membrane (Shirasu Porous Glass) Emulsification Technique

HAJIME YUYAMA, TOMOHIRO HASHIMOTO, GUANG-HUI MA, MASATOSHI NAGAI, SHINZO OMI

Graduate School of Bio-Applications and Systems Engineering, Tokyo University of Agriculture and Technology, Koganei 184-8588, Japan

Received 22 October 1999; accepted 24 February 2000

ABSTRACT: The mechanism of the unique suspension polymerization of uniform monomer droplets, without coalescence and breakup during the polymerization, was investigated using styrene (S) as a monomer mixed with water-insoluble hexadecane (HD). The glass membrane (Shirasu Porous Glass, SPG) emulsification technique was employed for the preparation of uniform droplets. Depending on the pore sizes of the SPG membranes (1.0, 1.4, and 2.9 μm), polymer particles of an average diameter ranging from 5.6 to 20.9 μm were obtained with the coefficient of variation (CV) being close to 10%. The role of HD was to prevent the degradation of the droplets by the molecular diffusion process. Sodium nitrite was added in the aqueous phase to kill the radicals desorbed from the droplets (polymer particles), thereby suppressing the secondary nucleation of smaller particles. Each droplet behaved as an isolated locus of polymerization. With the presence of HD, the initial polymerization rate was proportional to 0.24th power of the benzoil peroxide (BPO) concentration. This peculiar behavior as compared with the ordinary suspension polymerization was explained by introducing the assumption that each droplet was composed of isolated compartments (cells) in which active polymeric radicals were dissolved in an S-rich phase and surrounded by a rather incompatible S/HD (continuous) phase. The average number of radicals in the droplet increased initially due to the separate existence of polymeric radicals in compartments. As the polymerization progressed, the HD-rich phase gradually separated, eventually forming macrodomains, which were visible by an optical microscope. The phase separation allowed polystyrene chains to dissolve in a more favorable S phase, and the homogeneous bulk polymerization kinetics took over, resulting in a gradual decrease of the average number of radicals in the droplet until the increase of viscosity induced the gel effect. When no HD was present in the droplets, the polymerization proceeded in accordance with the bulk mechanism except for the initial retardation by the entry of inhibiting radicals generated from sodium nitrite in the aqueous phase. J Appl Polym Sci 78: 1025–1043, 2000

Key words: suspension polymerization; SPG membrane; styrene droplet; uniform microsphere; phase separation

INTRODUCTION

Shirasu porous glass (SPG) emulsification is a unique technique for preparing fairly uniform polymeric microspheres and microcapsules. The coefficient of variation of the diameter (standard deviation/average diameter) is normally around 10% or even less. The membrane, commercially available from a 0.1 to 18-μm pore size, was fabricated by Nakashima et al.[1] After the base glass, composed mainly of Al_2O_3—SiO_2—CaO—B_2O_3, was heated again to 1173 K, a bicontinuous structure, the Al_2O_3—SiO_2 and CaO—B_2O_3 phase, was

Correspondence to: H. Yuyama, Corporate Research Division, NIPPON NSC Ltd., 1-6-5, Senba Nishi, Minoo, Osaka 562-8586, Japan (hajime.yuyama@nstarch.com).

Journal of Applied Polymer Science, Vol. 78, 1025–1043 (2000)

induced by spinodal decomposition. The latter phase ($CaO—B_2O_3$) was removed by acid washing, leaving the skeleton structure of the former phase ($Al_2O_3—SiO_2$). To prepare an oil-in-water (O/W) emulsion, the oil phase is pushed through the pores of the SPG membrane by applying a carefully controlled pressure. Because of the narrow pore-size distribution, the oil droplets are formed in a uniform state. Addition of water-insoluble substances such as hexadecane (HD) and lauryl alcohol provides further stability of the droplets by preventing the diffusional degradation process of the droplets.

The authors realized a potential versatility of this particular technique for the preparation of uniform polymer particles by subsequent suspension polymerization and microcapsules by employing a solvent-evaporation process of the droplets. For example, a formulation of a monomer, a crosslinking agent, and a poor solvent yielded porous polymer particles, whereas another consisting of a hydrophilic monomer and a hydrophobic poor solvent resulted in hollow spheres by removing the solvent afterward. Composite spheres were also prepared by dissolving an unreactive substance in the monomer–solvent mixture. Relatively large spheres of several micrometers in diameter provided an adequate scale for the investigation of the particle morphology, a clear advantage to the submicron-scale latex particles. The droplets were so stable, no breakup or coalescence during the polymerization, that virtually the same number of polymer particles as that of the initial droplets was observed, except for a slight shrinkage of the diameter because of the density difference between the monomer and the polymer. The emulsification of the oil-phase, suspending hydrophilic powders in it, is rather difficult due to the poor stability of the suspension and the tendency of the powders plugging up the pores. Uniform magnetite microcapsules were prepared by overcoming these obstacles by the solvent-evaporation process. All these developments and other progress have been introduced several times.[2–5]

Because the authors were so preoccupied with the versatility of the SPG membrane for preparing various kinds of sophisticated polymer particles, fundamental investigations such as the mechanism of uniform droplets formation[6] and how the polymerization will proceed have been set aside until recently. Generally, the mechanism of suspension polymerization involving hydrophobic monomers such as styrene (S), which is a good solvent for its polymer, have been regarded essentially as the same as those of the bulk or solution polymerization kinetics. Breakup and coalescence of the droplets during polymerization affected only the size distribution of final polymer beads. Karfas and Ray[7,8] proposed a mathematical model to simulate the evolution of suspension polymerization of partially water-soluble monomers such as methyl methacrylate (MMA) and vinyl acetate (Vac) by introducing the partition of the monomer between the droplets and the aqueous phase. They confirmed that bulk polymerization kinetics is sufficient to quantify the suspension polymerization of S in which the droplets of millimeter size normally possess 10^8 radicals.

One of the most significant features in our emulsion system is that virtually no breakup or coalescence of the droplets takes place throughout the suspension polymerization. This situation, although the droplet size is about two orders larger, reminds the authors of a unique miniemulsion polymerization of S reported by Miller et al.[9,10] They found that almost all the initial miniemulsion droplets were converted to polymer particles when they dissolved polystyrene having SO_4^- groups at both ends in the droplets. They concluded that the droplets behaved as though they were monomer-swollen seed polymer particles in emulsion polymerization, and the miniemulsion process was regarded as a growth period. A water-soluble initiator, potassium persulfate, was used, and they did not neglect the desorption of radicals from the polymer particles to the aqueous phase when they tried to elucidate the reaction mechanism. In other words, this mechanism involves the exchange of radicals across the interface of the polymer particles.

Besides the larger droplet size, the presence of water-insoluble HD in our emulsion system prevents the desorption of radicals from the droplets, and the addition of sodium nitrite in the aqueous phase as a radical scavenger makes the reentry of radicals from the aqueous phase practically impossible. These unique features imply that the droplets are regarded as the loci of the compartmentalized polymerization system first proposed by Haward[11] and later extended by Blackley[12] with rigid mathematical developments. However, Blackly pointed out that the compartmentalized polymerization system can be applied only to the loci in which 0.01–2 radicals normally coexist with 10 radicals utmost. In our polymer particles, the average number of radicals is 10^{6-7}, as shown in the later part.

In this article, the mechanism of this unique suspension polymerization that takes place in the

isolated droplets was investigated. It is shown that the initial behavior of the polymerization is different depending on the presence of HD in the droplets. The S/HD mixture was rather a poor cosolvent for polymeric radicals, and a concept of compartmentalized radicals was proposed to elucidate the peculiar mechanism. Without the presence of HD, the polymerization behaved as though it were an ordinary bulk polymerization process.

EXPERIMENTAL

Materials

Sodium lauryl sulfate (SLS; Wako Pure Chemical Co., Ltd., Tokyo, Japan) and poly(vinyl alcohol) (PVA; degree of hydrolysis, 87.8 mol %; average degree of polymerization, 1725; Kuraray Co., Ltd., Tokyo, Japan), composing a mixed stabilizer, were used as received without further purification. S and HD were reagent grade and used as received. Benzoyl peroxide (BPO) with a 25 wt % moisture content (Kishida Chemical Co. Ltd., Tokyo, Japan) was reagent grade and used as an initiator. Sodium nitrite ($NaNO_2$) was reagent grade (Kanto Chemical Co., Ltd., Tokyo, Japan) and used as a water-soluble inhibitor to prevent the secondary nucleation of polymer particles in the aqueous phase. Twice-distilled and deionized water (DII) was used for the preparation of aqueous solutions. Nitrogen was a high-purity grade.

Emulsification

A particular apparatus for emulsification with a microporous glass (MPG; Ise Chemical Co., Ltd.) module was already presented in our previous report.[3] SPG membranes were immersed in an SLS solution and treated with ultrasonification (Branson Sonic Model B-5200J-4) prior to use so that the surface may be thoroughly wetted with the aqueous phase. The dispersion phase, a mixture of S and HD dissolving a small amount of BPO, was stored in a pressure-tight storage tank and allowed to permeate through the membrane under an appropriate pressure in the recirculating flow of the continuous phase, an aqueous solution of the stabilizers, and the water-soluble inhibitor. The droplets were suspended in the continuous phase and stored in an emulsion storage tank with a gradual increase of the droplet numbers. After the half-volume of the dispersion phase was emulsified, the emulsion was withdrawn from the storage tank and served for polymerization. A more detailed description can be found elsewhere.[1–6]

Table I Standard Recipe of Emulsification and Polymerization

1. Continuous phase	
Water (DII)	450 g
Poly(vinyl alcohol) (PVA)	6.02 g
Sodium lauryl sulfate (SLS)	0.60 g
Sodium nitrite ($NaNO_2$)	0.00, 0.20g
2. Dispersion phase	
Styrene (S)	20 g
Hexadecane (HD)	0.0, 5.0 g
Benzoyl peroxide (BPO)[a]	0.15, 0.30, 0.45, 0.60 g
3. Emulsification	
SPG membrane pore size	1.0, 1.4, 2.9 μm
Applied pressure[b]	0.13, 0.30, 0.49 kgf/cm^2
Circulation flow rate[c]	330 mL/min
4. Polymerization	
Reaction temperature	348 K
Reaction time	26 h
Agitation rate	122 rpm

[a] 25 wt % moisture content.
[b] Nitrogen pressure applied to the pressure bottle.
[c] Recirculation rate of the continuous phase in which the droplets were gradually released.

Polymerization

As the initiator, BPO, was already mixed with the monomer in the dispersion phase, efficient operation was required to minimize the idle time. Five hundred grams of the emulsion was transferred to an ordinary glass separator flask, and gentle bubbling of nitrogen into the emulsion was followed with mild agitation. After 1 h, the bubbling nozzle was removed from the emulsion, the ingredients were heated to the reaction temperature at 75°C and polymerized for 26 h under a nitrogen atmosphere. After the polymerization, the polymer particles were removed from the serum by centrifugation, washed with methyl alcohol, and dried under a vacuum. A small amount of the samples was withdrawn periodically from the reactor and was short-stopped by adding methyl ethylhydroquinon as an oil-soluble inhibitor and stored in an ice bath. Table I indicates the standard recipe used for all the reactions.

Analysis

Percent conversion of S was measured with headspace gas chromatography (HS-GC; HS module:

Table II Properties of Obtained Monomer Droplets Prepared with Different SPG Pore Sizes and Their Polymerized Particles

	Emulsion Droplets			Polymer Particles		
SPG Pore Size (μm)	$\bar{d}n$[a] (μm)	CV[b] (%)	No. Droplets (/L)[c]	$\bar{d}n$[d] (μm)	CV (%)	No. Particles (/L)[c]
2.9	20.9	11.9	3.73×10^9	19.6	15.7	4.53×10^9
1.4	8.9	11.7	6.25×10^{10}	8.3	12.2	6.38×10^{10}
1.0	5.6	8.2	2.51×10^{11}	5.0	9.2	2.80×10^{11}

Monomer droplets contained 10.3 mol % of HD and 0.0991 mol/L of BPO based on the dispersion phase. The continuous phase contained 0.2 g of sodium nitrite as a water-soluble inhibitor.
[a] Number-average droplet size.
[b] Coefficient of variation.
[c] Number in the total emulsion.
[d] Number-average particle size.

Perkin–Elmer HS-40; GC module: Hewlett–Packard 5890 Series II). The injecting samples were prepared by adding a known amount of toluene as an external standard and then diluted with 10 mL of tetrahydrofuran (THF).

Emulsion droplets before and during the polymerization and polymer particles were observed with an optical microscope (Nikon Optiphoto 200). Diameters of several hundred droplets or particles were counted to calculate average diameters and the coefficient of variation (CV = standard deviation/average diameter $\times$ 100%). General features of the polymer particles were observed with an SEM (Hitachi S-2500CX).

Average molecular weight and molecular weight distribution were measured with gel permeation chromatography (GPC; Waters 510/410), employing THF as an elution solvent. The columns were calibrated with nine standard polystyrene samples.

RESULTS AND DISCUSSION

Polymerization of Monomer Droplet Including HD (HD System)

Effects of Monomer Droplet Size

Average diameters and the CV of the obtained monomer droplets and polymer particles are listed in Table II with the SPG pore size. Figure 1 shows the conversion–time curves for polymerization, where the monomer droplet containing 10.3 mol % of HD and a 0.0726 mol/L-oil phase of BPO were prepared with different pore sizes of the SPG membrane: 1.0, 1.4, and 2.9 μm. The conversion–time curves show a similar conversion profile regardless the average size of the monomer droplets. All curves were found to have the same kinetics features. The polymerization rate for different monomer droplet sizes is shown in Figure 2. All runs showed the same general behavior during the polymerization. The rate reached a maximum, decreased slowly, increased again for a short period, and decreased gradually until the end of the reaction. The following discussion is intended to provide a basic understanding of the polymerization rate curves, which will then be

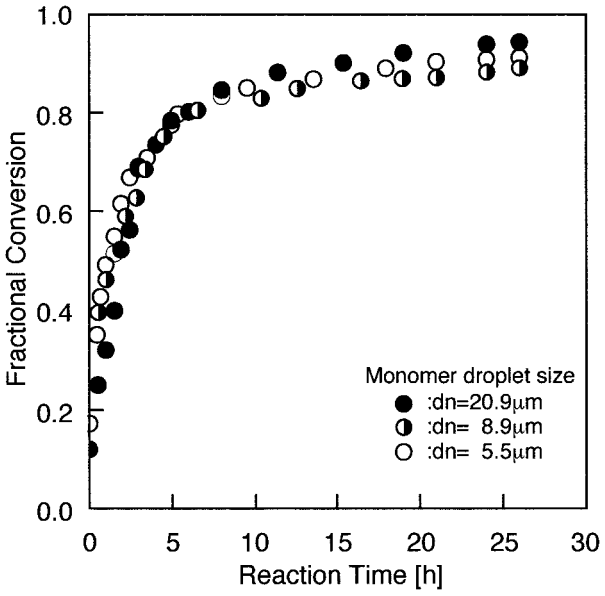

Figure 1 Conversion versus time curves for polymerization of S droplets in the presence of hexadecane initiated by 0.0726 mol/L-oil phase of BPO and at three different number-average droplet sizes: (●) 20.9 μm; (◑) 8.9 μm; (○) 5.5 μm.

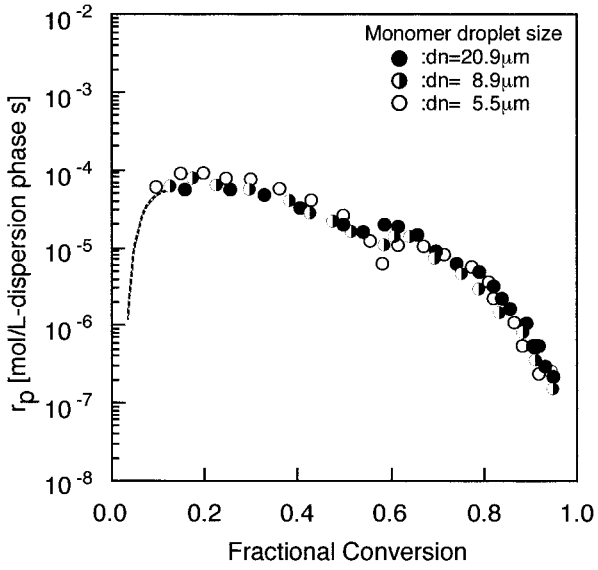

Figure 2 Polymerization rate versus fractional conversion curves for S droplets in the presence of hexadecane initiated by 0.0726 mol/L-oil phase of BPO and at three different number-average droplet sizes: (●) 20.9 μm; (◑) 8.9 μm; (○) 5.5 μm.

discussed in more detail in a later section. The first increase in the rate of polymerization until 0.1 of the fractional conversion is attributed to the generation and growth of the polymeric radicals in the droplets. Let us define these droplets as *polymer particles* although they are several orders larger than those in conventional emulsion polymerization. This period lasted 0.5–1.0 h from the start. The second stage continued until 0.5–0.6 of the fractional conversion, where the polymerization rate started to decrease as a result of the steady drop in the monomer concentration in the polymer particles. This decrease in monomer concentration in the particles continued until the final conversion was achieved. At the end of this stage, the rate again increased to a second maximum. This is attributed to the well-known gel effect: acceleration due to the viscosity increase within the growing particles. Finally, at high conversion, the polymerization rate decreased again.

In this system, the continuous phase can be regarded as a sink for active radicals since a water-soluble inhibitor was added to suppress the nucleation of secondary particles. Stability of the monomer droplets was maintained during the polymerization because of the uniform size and the presence of a water-insoluble substance, HD (solubility in water: 9.0×10^{-8} wt % at 283 K), which prevents the monomer from diffusing out of the droplet. Indeed, the droplets were so stable that all the droplets were converted to polymer particles and did not serve as the reservoirs of monomers as in the case of conventional emulsion polymerization.

Virtually, neither the coalescence nor the breakup of the droplets took place—only a small shrinkage in volume due to the conversion of monomer to polymer.[13] The number of polymer particles was expected to remain equal to the initial number of monomer droplets before the polymerization. Table II shows that the number-average particle size and particle number are not significantly different. In Figure 3, the number of polymer particles calculated from the average particle size is shown as a function of the fractional monomer conversion, providing substantial evidence of the discussion described above. Also, Figure 4 shows that the size distributions of the initial droplets and the final polymer particles all revealed similar curves except the slight decrease in the size of polymer particles. These results suggest that the polymerization mechanism of the HD system is not dependent on the initial droplet size ranging from 5.6 to 20.9 μm as a locus of polymerization.

Effects of Initiator Concentration

Figure 5 shows the conversion–time curves for the polymerization of monomer droplets prepared with a 1.0-μm pore size, where the initiator con-

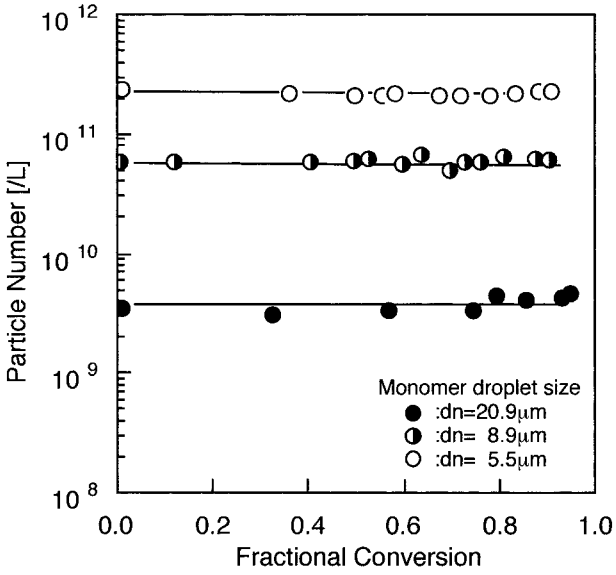

Figure 3 Particle number during polymerization of S droplets in the presence of hexadecane at three different number-average droplet sizes: (●) 20.9 μm; (◑) 8.9 μm; (○) 5.5 μm.

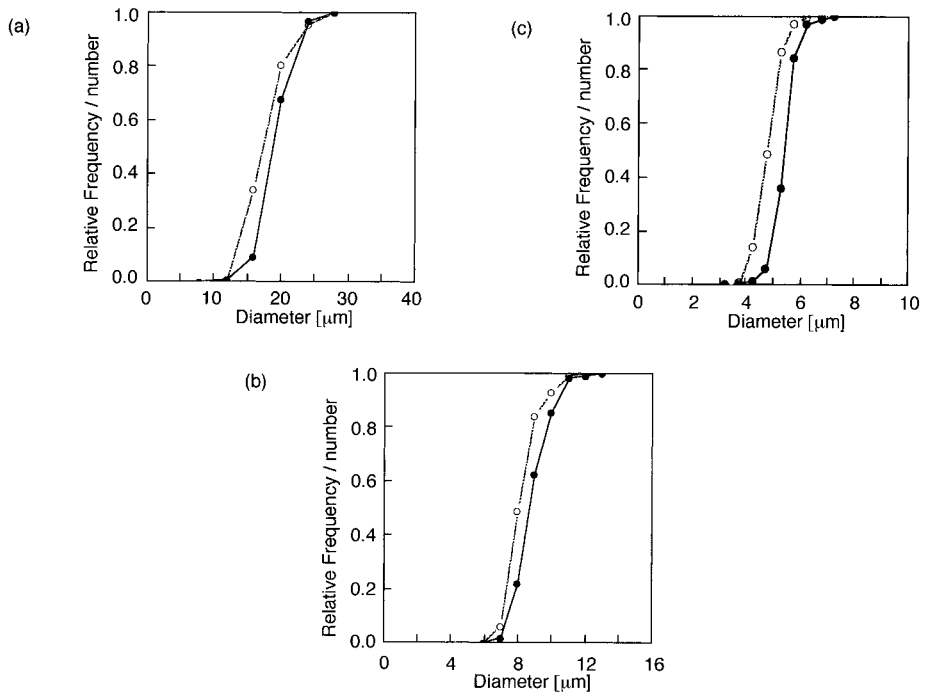

Figure 4 Measured particle-size distribution of S droplets in the presence of hexadecane: (a) $dn = 20.9$ μm; (b) $dn = 8.9$ μm; (c) $dn = 5.5$ μm. (●) Before polymerization; (○) after polymerization.

centration was varied from 0.0217 to 0.0726 mol/L-oil phase. The overall polymerization rate increased with the amount of initiator. Figure 6 shows logarithmic plots of the number of polymer particles and the initial polymerization rate versus the initiator concentration. The rate of polymerization varied to the 0.24th power of the initiator concentration. The number of particles did

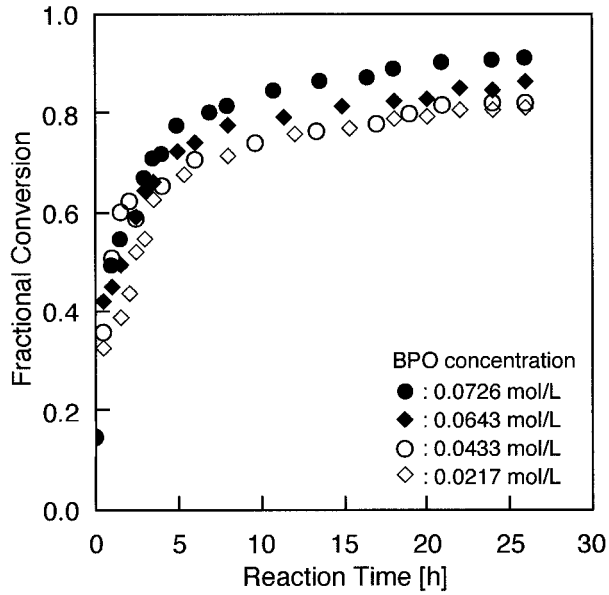

Figure 5 Conversion versus time curves for polymerization of S droplets in the presence of hexadecane prepared using 1.0 μm of SPG and initiated using 0.0217, 0.0433, 0.0643, and 0.0726 mol/L-oil phase BPO.

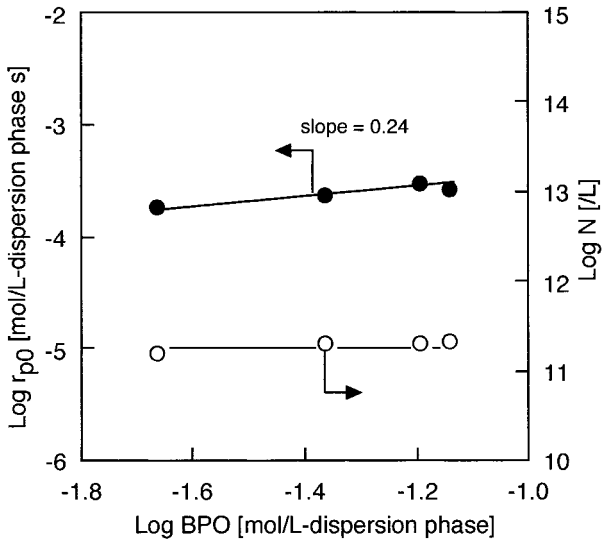

Figure 6 Log–log plot of the number of particles and first maximum polymerization rate versus initiator concentration for polymerization of S droplets in the presence of hexadecane prepared using 1.0 μm of SPG.

Table III Effect of BPO Concentration in the Dispersion Phase (HD System)

	Emulsion Droplets			Polymer Particles				
BPO (mol/L)[a]	$\bar{d}n$[b] (μm)	CV[c] (%)	No. Droplets (/L)[d]	$\bar{d}n$[e] (μm)	CV (%)	No. Particles (/L)[d]	$\bar{M}_n$[f]	$\bar{M}_w$[g]
0.0726	5.6	8.2	2.51×10^{11}	5.0	9.2	2.80×10^{11}	2.12×10^4	2.80×10^4
0.0643	5.8	8.4	2.26×10^{11}	5.3	9.1	2.39×10^{11}	2.31×10^4	3.07×10^4
0.0433	6.1	8.6	1.92×10^{11}	5.3	9.9	2.42×10^{11}	2.11×10^4	3.15×10^4
0.0217	6.1	9.8	1.95×10^{11}	5.9	10.0	1.81×10^{11}	2.87×10^4	4.14×10^4

Monomer droplets were prepared with a 1.0-μm pore size and contained 10.3 mol % of HD based on the dispersion phase. The continuous phase contained 0.2 g of sodium nitrite as a water-soluble inhibitor.

[a] Concentration in the dispersion phase.
[b] Number-average droplet size.
[c] Coefficient of variation.
[d] Number in the total emulsion.
[e] Number-average particle size.
[f] Number-average molecular weight.
[g] Weight-average molecular weight.

not change with the initiator concentration. The results listed in Table III indicate that both the droplets and final polymer particle size did not significantly change before and after polymerization. This implies that the formation of the initial monomer droplets slightly depended on the BPO concentration, probably due to the minor changes inflicted to the interfacial tension, viscosity, and hydrophobicity. The low dependence of the initial polymerization rate on the initiator concentration (0.24th power) compared to the square-root dependence in the case of ordinary bulk polymerization[14] is discussed in the later section dealing with the mechanism of polymerization.

The number- and the weight-average molecular weight of the polymers composing the final polymer particles are listed in Table III. In Figure 7, the number- and weight-average degree of polymerization is plotted against the fractional conversion when the monomer droplets were prepared with a pore size of 1.42 μm, and the concentration of BPO was 0.0726 mol/L-oil phase. It can be seen that the degree of polymerization ($\bar{P}n$, $\bar{P}w$) decreased steadily and decreased even more rapidly after the fractional monomer conversion exceeded 0.6. The decrease of the number-average molecular weight during polymerization is similar to that obtained by Alduncin and Asua.[15] They reported that this decrease was due to chain transfer to the initiator, which counteracted the influence of the gel effect in the study of miniemulsion polymerization of S with HD (2 wt %) initiated by BPO.

Since there is no radical entry from the aqueous phase because of the presence of a water-soluble inhibitor and virtually no coalescence or breakup of the droplets, each monomer droplet behaves as being an isolated locus. Let us first assume that the molecular weight was controlled by the bulk polymerization kinetics, that is, termination by the combination of two polymeric radicals and the chain transfer of radicals to HD; chain transfer to the monomer can be neglected because the chain-transfer coefficient of S is of the order of 10^{-5} compared to 10^{-2} of HD.[16] From the bulk polymerization kinetics, the number-aver-

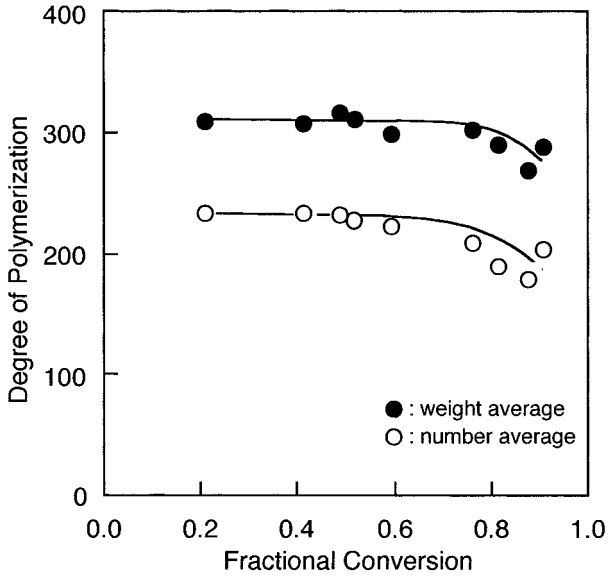

Figure 7 Degree of polymerization during the polymerization of S droplets in the presence of hexadecane prepared using 1.4 μm of SPG: (○) number-average; (●) weight-average.

Table IV Properties of Obtained Monomer Droplets Without HD Prepared with Different SPG Pore Sizes and Their Polymerized Particles

	Emulsion Droplets			Polymer Particles		
SPG Pore Size (μm)	$\bar{d}n$[a] (μm)	CV[b] (%)	No. Droplets (/L)[c]	$\bar{d}n$[d] (μm)	CV (%)	No. Particles (/L)[c]
2.9	28.2	28.4	1.25×10^9	27.1	19.8	1.21×10^9
1.4	8.7	12.7	5.16×10^{10}	7.4	16.0	6.11×10^{10}
1.0	5.7	14.4	1.80×10^{11}	5.0	16.5	1.78×10^{11}

Monomer droplets contained 0.1170 mol/L of BPO based on the dispersion phase. The continuous phase contained 0.2 g of sodium nitrite as a water-soluble inhibitor.

[a] Number-average droplet size.

[b] Coefficient of variation.

[c] Number in the total emulsion.

[d] Number-average particle size.

age degree of polymerization can be estimated. The rate constants of propagation (k_p = 413 L mol^{-1} s^{-1}) and termination [k_t 1.11(10^8) L mol^{-1} s^{-1}] by recombination for S at 348 K were obtained from the literature.[16,17] The decomposition rate constant of BPO (k_d) is 1.83×10^{-5} s^{-1}.[17] The volume unit, L, refers to the volume of the oil phase.

From the experimental recipe, the rate of initiation (r_i) is 1.35×10^{-6} mol L^{-1} s^{-1}, where the initial concentration of S, HD, and BPO are 6.58, 0.757, and 0.0726 mol/L, respectively. Then, the initial rate of polymerization (r_p) is given as 3.00×10^{-4} L^{-1} s^{-1}. This value is in good agreement with the observed value shown as the point located at the extreme right in Figure 6.

The initial number-average degree of polymerization controlled by the combination of radicals ($\bar{p}_{n0,t}$) can be calculated as 444, whereas the initial number-average degree of polymerization dominated by the chain transfer to HD ($\bar{p}_{n0,tr}$) is given as 870. With these two values being combined, the overall degree of polymerization can be estimated as

$$\bar{P}_{n0} \cong \bar{p}_{n0} = \frac{1}{1/\bar{p}_{n,t} + 1/\bar{p}_{n,tr}} = \frac{1}{1/444 + 1/870} = 294$$

$\bar{p}_{n0,t}$ and $\bar{P}_{n0}$ are larger than is the initially observed value of 207 as shown in Figure 7. If one assumes that the termination in the droplets takes place between one polymeric radical and a small radical (initiator radical) rather than a transferred radical, then the value will be 222 and in good agreement with the observed value. The bulk polymerization mechanism was not valid to estimate the number-average degree of polymerization.

Polymerization of Monomer Droplet Without HD (Non-HD System)

Effects of Monomer Droplet Size

To study the effect of HD on the polymerization, the monomer droplets without HD were polymerized. In this system, defined as the non-HD system, the active radicals and monomers as well are subject to diffuse from the particles to the continuous phase during the polymerization; however, the continuous phase is a sink for the active radicals as in the case of the HD system.

The average diameter and CV of the S monomer droplets and the polymer particles are listed in Table IV with the SPG pore size. The absence of HD is reflected on the high CV values when the largest pore size (2.9 μm) was employed for the emulsification. Figure 8 shows the conversion–time curves of the polymerization, where the monomer droplets containing BPO, 0.117 mol/L-oil phase, were prepared with the same pore sizes of the SPG membranes as in the HD system. Compared with the HD system (Fig. 1), the conversion–time curves showed a different conversion profile. From the start to 0.3 of the fractional conversion, it was found that the polymerization proceeded slowly as though in an induction period regardless of the size of the monomer droplets, and this period lasted 2.0 h from the starting time. The polymerization rates for different monomer droplet sizes are shown in Figure 9. The

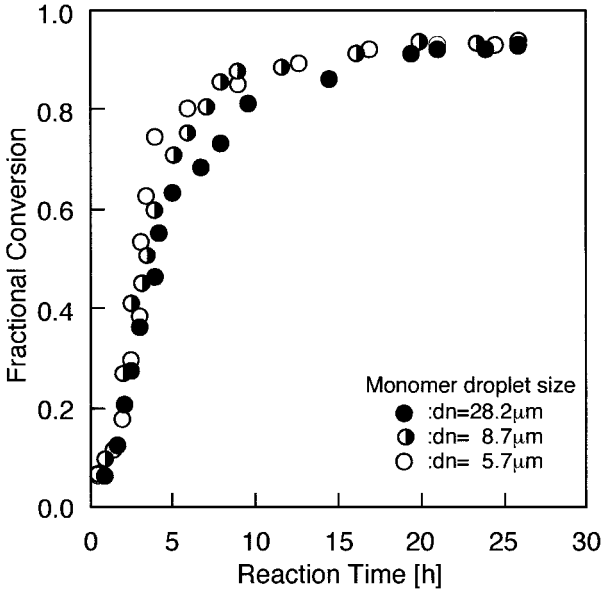

Figure 8 Conversion versus time curves for polymerization of S droplets in the absence of hexadecane initiated by 0.117 mol/L-oil phase of BPO and at three different number-average droplet sizes: (●) 28.2 μm; (◑) 8.7 μm; (○) 5.7 μm.

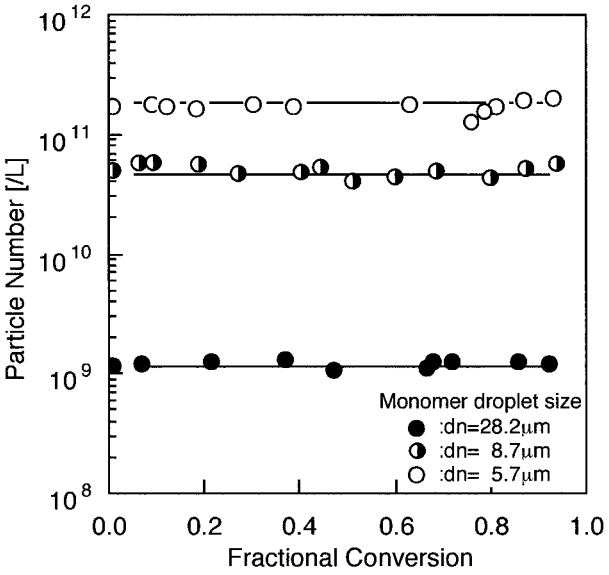

Figure 10 Particle number during the polymerization of S droplets in the absence of hexadecane at three different number-average droplet sizes: (●) 28.2 μm; (◑) 8.7 μm; (○) 5.7 μm.

overall polymerization rate curves showed the same general behavior except for the appearance of the gel effect. The polymerization rate reached the maximum slower than that of the HD system, stayed almost constant for a short period, increased again due to the gel effect, and decreased gradually until the end of the reaction. From the fractional conversion 0.5–0.7, the smaller droplets appeared to exhibit a more prominent gel effect, and it started at a lower fractional conversion than that of the larger droplets.

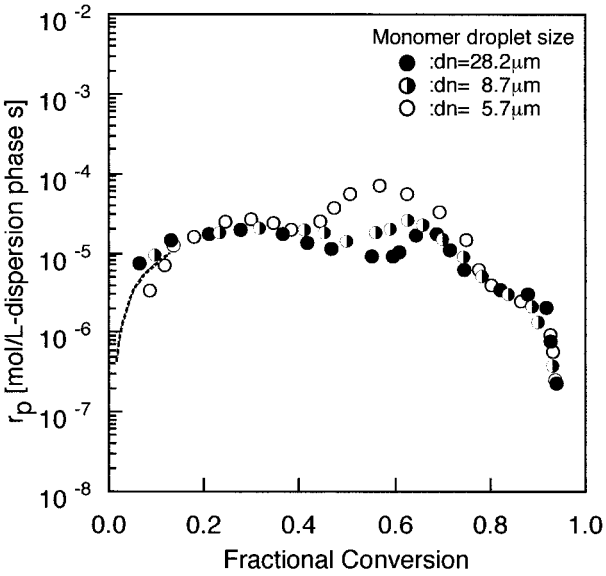

Figure 9 Polymerization rate versus fractional conversion curves for S droplets in the absence of hexadecane initiated by 0.117 mol/L-oil phase of BPO and at three different number-average droplet sizes: (●) 28.2 μm; (◑) 8.7 μm; (○) 5.7 μm.

In the liquid–liquid dispersion systems, the possibility that the recirculating flow exists in the droplets (hence, enhanced mobility of molecules) is governed by the bond number ($g\Delta\rho d_p^2/\gamma$), where g is the acceleration rate by gravity; $\Delta\rho$, the density difference between the continuous and the dispersion phase; d_p, the average diameter of the droplet; and γ, the interfacial tension. Although no appreciable flow may actually exist in our micron-scale droplet system, still it may be reasonable to assume that the radicals in the smaller droplets are less mobile. The consequence will be an accumulation of the radicals, inducing an enhanced gel effect in the earlier stage of the reaction.

In Figure 10, the number of polymer particles is shown as a function of the fractional monomer conversion. The number of polymer particles did not change during the polymerization as in the HD system. Figure 11 shows the size distribution of the initial droplets and the final polymer particles. Comparison of the CV values in Tables II and IV indicates that the size distributions were broader with the runs without HD, in particular,

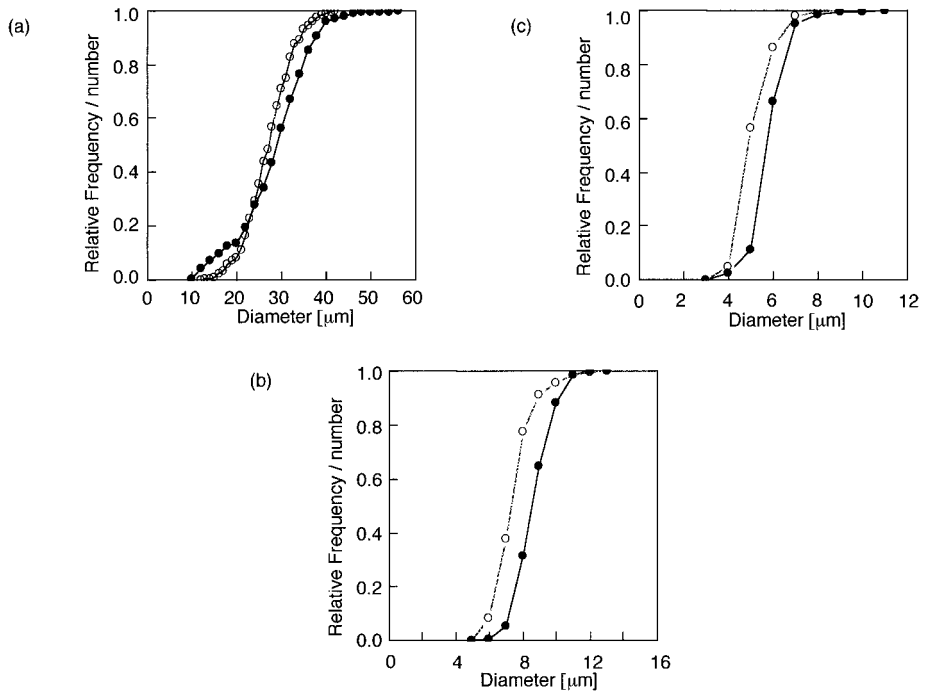

Figure 11 Measured particle-size distribution of S droplets in the absence of hexadecane prepared by three different SPG pores: (a) 1.0 μm of SPG pore; (b) 1.4 μm of SPG pore; (c) 2.9 μm of SPG. (●) Before polymerization; (○) after polymerization.

when the largest pore size (2.9 μm) was employed. The distributions shown in Figures 4(b) and 11(b) were plotted against the same scale of the horizontal axis, demonstrating a broader size distribution of the latter. The reason for a broader distribution of the initial droplet size without HD was already presented in our report.[6] The droplet size and its distribution were significantly affected by the hydrophobicity of the dispersion phase, which depends on the amount of HD. These results suggest that the polymerization mechanism without HD was not dependent on the initial droplet size from 5.7 to 21.7 μm, except during the period of the gel effect.

Effects of Initiator Concentration

Figure 12 shows the conversion–time curves for the polymerization of the monomer droplets prepared with a 1.0-μm pore size, where the initiator concentration was varied from 0.0299 to 0.1170 mol/L-oil phase. The polymerization rate increased with the amount of initiator significantly. Figure 13 shows a logarithmic plot of the number of final polymer particles and the initial polymerization rate at the point of the first maximum versus initiator concentration. This figure shows that the polymerization rate was proportional to the 0.48th power of the initiator concentration, except the point of the lowest concentration. The number of particles did not change with the ini-

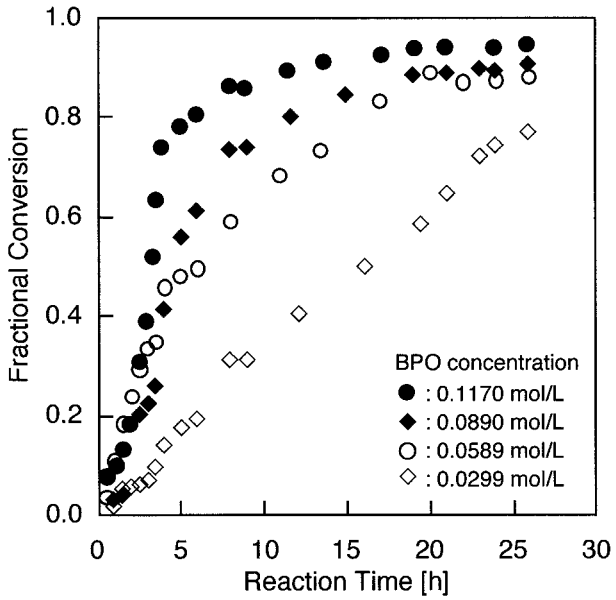

Figure 12 Conversion versus time curves for polymerization of S droplets in the absence of hexadecane prepared by 1.0 μm of SPG and initiated using 0.0299, 0.0589, 0.0890, and 0.1170 mol/L-oil phase BPO.

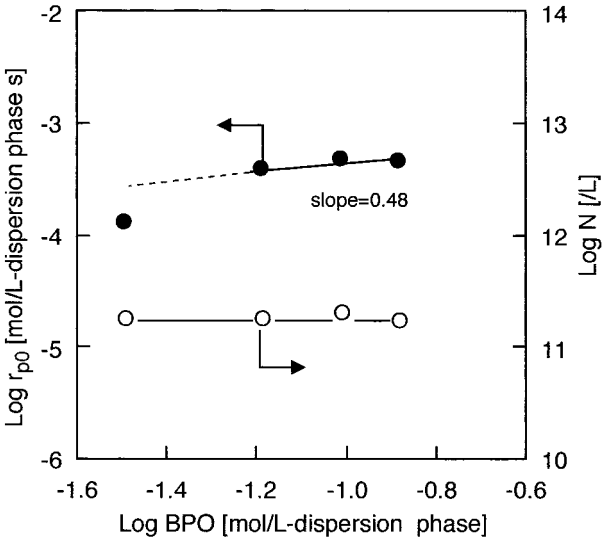

Figure 13 Log–log plot of the number of particles and first maximum polymerization rate versus initiator concentration for polymerization of S droplets in the absence of hexadecane prepared using 1.0 μm of SPG.

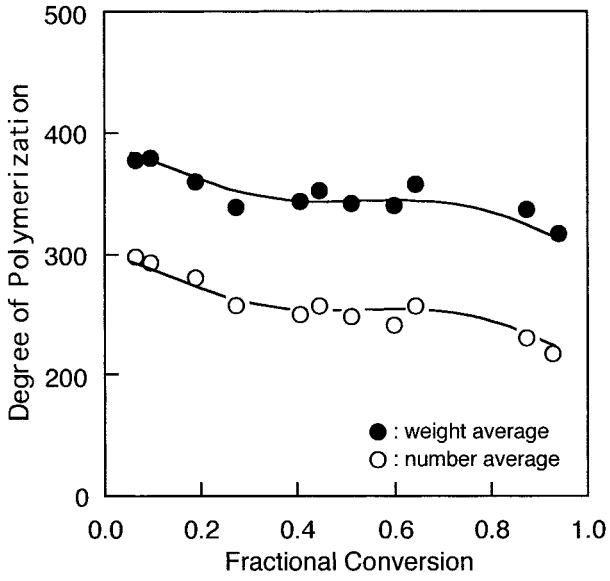

Figure 14 Degree of polymerization during polymerization of S droplets in the absence of hexadecane prepared using 1.4 μm of SPG: (○) number-average; (●) weight-average.

tiator concentration as in the case of the HD system. Table V shows that the average diameter and CV values of the initial droplets and the final polymer particles did not depend on the BPO concentration. As shown in the other tables (II–IV), the size distribution of the final polymer particles became broader than those of the initial monomer droplets.

In Figure 14, the number- and weight-average degree of polymerization are plotted against the fractional conversion when the monomer droplets were prepared with a pore size of 1.42 μm, and the concentration of BPO was 0.117 mol/L-oil phase. By comparing two pairs of figures, Figures 2 and 9 and Figures 7 and 14, respectively, the effect of HD in the droplets to the mechanism of the polymerization can be considered as follows: Without the presence of HD, a slow increase of the polymerization rate (Fig. 9) and an initial decrease of the degree of polymerization (Fig. 14) were observed. Fitch[18] suggested that $NaNO_2$ as a water-soluble inhibitor eventually generates nitrogen dioxide and nitric oxide which deactivate

Table V Effect of BPO Concentration in the Dispersion Phase (Non-HD System)

	Emulsion Droplets			Polymer Particles				
BPO (mol/L)[a]	$\bar{d}n$[b] (μm)	CV[c] (%)	No. Droplets (/L)[d]	$\bar{d}n$[e] (μm)	CV (%)	No. Particles (/L)[d]	$\bar{M}_n$[f]	$\bar{M}_w$[g]
0.1170	5.7	14.4	1.88×10^{11}	5.0	16.5	1.78×10^{11}	2.30×10^4	3.51×10^4
0.0890	5.9	12.8	1.61×10^{11}	4.9	16.3	2.09×10^{11}	2.45×10^4	3.87×10^4
0.0589	5.6	12.7	1.90×10^{11}	4.8	13.6	2.29×10^{11}	2.85×10^4	4.50×10^4
0.0299	6.0	12.9	1.18×10^{11}	4.9	16.3	2.14×10^{11}	2.74×10^4	6.08×10^4

Monomer droplets were prepared with a 1.0-μm pore size. The continuous phase contained 0.2 g of sodium nitrite as a water-soluble inhibitor.

[a] Concentration in the dispersion phase.
[b] Number-average droplet size.
[c] Coefficient of variation.
[d] Number in the total emulsion.
[e] Number-average particle size.
[f] Number-average molecular weight.
[g] Weight-average molecular weight.

Table VI Effect of HD Content and $NaNO_2$ Content on Polymerization

		Emulsion Droplets			Polymer Particles					
HD (mol %)[a]	$NaNO_2$ (mol/L)[b]	$\bar{d}n$[c] (μm)	CV[d] (%)	No. Droplets (/L)[e]	$\bar{d}n$[f] (μm)	CV (%)	No. Particles (/L)[e]	$\bar{M}_n$[g] ($\times 10^4$)	$\bar{M}_w$[h] ($\times 10^4$)	Dp[i]
0.0	0.005	8.7	12.7	5.16×10^{10}	7.4	16.0	6.11×10^{10}	2.30	3.51	1.52
0.0	0.000	9.8	18.3	3.43×10^{10}	6.0	17.9	1.11×10^{11}	2.68	5.87	2.19
10.3	0.005	8.9	11.7	6.25×10^{10}	8.3	12.2	6.38×10^{10}	2.11	2.80	1.33
10.3	0.000	9.7	13.1	4.71×10^{10}	7.6	13.9	7.81×10^{10}	2.34	3.98	1.69

Monomer droplets of the non-HD system contained 0.117 mol/L of BPO based on the dispersion phase. Monomer droplets of the HD system contained 0.0276 mol/L of BPO based on the dispersion phase. All monomer droplets were prepared with a 1.4-μm pore size.

[a] HD content based on the dispersion phase.
[b] Concentration in the total emulsion.
[c] Number-average particle size.
[d] Coefficient of variation.
[e] Number in the total emulsion.
[f] Number-average particle size.
[g] Number-average molecular weight.
[h] Weight-average molecular weight.
[i] Molecular weight dispersity of polymer (M_w/M_n).

water-soluble radicals. He also pointed out that these radicals are soluble in a hydrophobic medium, hence capable of inhibiting the polymerization without HD. Then, the polymeric radicals in the S droplets will be more susceptible to be short-stopped by these species. This may explain the profile of a gradual increase of the polymerization rate in Figure 9 and an initial decrease of the degree of polymerization in Figure 14. Notice that the initial value of the degree of polymerization was higher than that observed in Figure 7 (even though the initiator concentration was slightly higher, 0.117–0.0726 mol/L-oil phase, implying that the mechanism of the non-HD system followed the bulk polymerization mechanism except the initial entry of inhibiting radicals from the aqueous phase. As the amount of polymers was accumulating in the droplets, the droplets gained enough hydrophobicity as in those with HD, the entry of the inhibiting radicals became less enhanced, and the polymerization in the droplets proceeded similar to that of the HD system.

Effect of Sodium Nitrite on the Polymerization With and Without HD

As described above, it was suggested that sodium nitrite as a water-soluble inhibitor affected the polymerization of the monomer droplets with and without HD initiated by an oil-soluble initiator. In this section, the effect of $NaNO_2$ on the polymerization of both the HD and non-HD systems will be discussed.

Data of the obtained monomer droplets and polymer particles are listed in Table VI with the connections of HD and $NaNO_2$, which were extracted from the data in Tables II and IV. Conversion–time curves for the four polymerization systems are shown in Figure 15, in which the corresponding runs in Figures 1 and 8 were in-

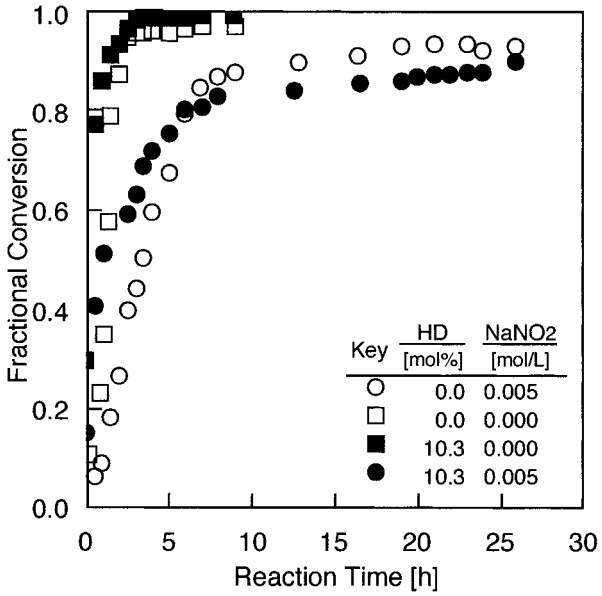

Figure 15 Conversion versus time curves for polymerization of S at four different recipe conditions: (○) HD 0.0 mol %, $NaNO_2$ 0.005 mol/L; (□) HD 0.0 mol %, $NaNO_2$ 0.000 mol/L; (■) HD 10.3 mol %, $NaNO_2$ 0.000 mol/L; (●) HD 10.3 mol %, $NaNO_2$ 0.005 mol/L.

cluded. For the runs without $NaNO_2$ (square symbols), the conversion–time curve showed a similar tendency, and the polymerization rates were faster than were those in the runs with $NaNO_2$ (circular symbols) regardless the presence of HD. The number- and the weight-average molecular weight of the polymers composing the final polymer particles are listed in Table VI. For the runs without $NaNO_2$, the molecular weight distributions were broader than were those prepared with $NaNO_2$. In particular, the non-HD run revealed a broader distribution.

The sizes of the monomer droplets and polymer particles, listed in Table VI, showed that the monomer droplet sizes and the size distributions without $NaNO_2$ were larger and broader than were those prepared with $NaNO_2$. This implies the interaction of sodium nitrite with the mixed stabilizer, although the mechanism has yet to be understood. The final polymer particle size of the runs without $NaNO_2$ was somewhat smaller than were the runs with $NaNO_2$. Moreover, the number of particles of the runs with no $NaNO_2$ increased remarkably, compared with the number of droplets. These results imply a scenario that without the addition of $NaNO_2$ the secondary nucleation of polymer particles took place, resulting in the increased polymerization rate and molecular weight and broadening of the molecular weight distribution.

In Figure 16, the number of polymer particles formed without $NaNO_2$ is shown as a function of the fractional conversion. The run without HD changed significantly during the polymerization,

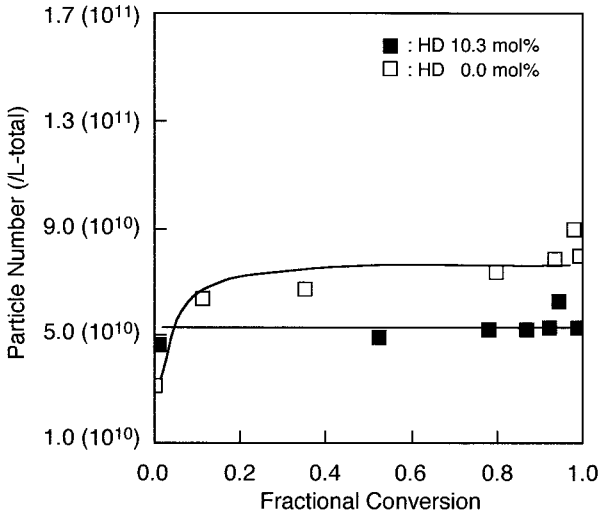

Figure 16 Particle number during the polymerization of S droplets in the absence of water-soluble inhibitor: (□) HD 0.0 mol % ; (■) HD 10.3 mol %.

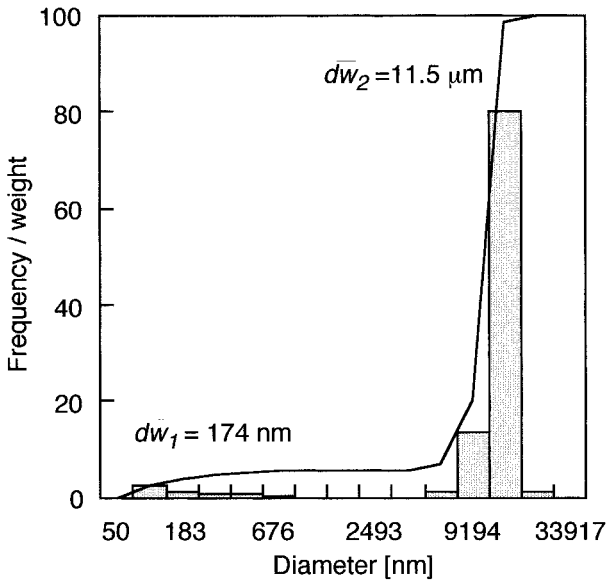

Figure 17 Measured polymer particle-size distribution of S droplets in the absence of neither HD nor $NaNO_2$.

especially at the initial polymerization stage, from the start to 0.2 of the fractional conversion. However, for the run with HD, the number of polymer particles did not change remarkably as in the HD system, as shown in Figure 10. The particle-size distribution of the run prepared without HD and $NaNO_2$ is given in Figure 17. The first peak of the weight-average particle size is 174 nm and the second peak is 11.5 μm, yielding a bimodal distribution curve. It is confirmed that the nucleation of secondary particles occurred by the desorption of the monomer and radicals from the particles to the aqueous phase at the early stage of the polymerization.

These results indicate that the addition of a water-soluble inhibitor together with the oil-soluble initiator retarded the polymerization of the monomer droplets without HD in the initial stage of the polymerization. For both systems with and without HD, the water-soluble inhibitor caused a delay of the overall polymerization by consuming the radicals in the monomer droplets as well as in the aqueous phase.

Mechanism of Polymerization

From the results and the discussions above, it is apparent that the monomer droplets served as the main loci of initiation, propagation, and termination of free radicals. This situation corresponds closely to the approach adopted by Sudol

et al.[19] to produce monodisperse latexes through the successive seeding processes based upon the concept of polymerization within the locus prepared in advance. Furthermore, the miniemulsion polymerization is defined as the polymerization in the monomer droplets dispersed in the initial emulsion, where the initial droplet-size distribution is reflected in the final polymer particle-size distribution. Tang et al.[20] studied the differences in the polymerization kinetics of S between a conventional emulsion and a miniemulsion stabilized with SLS together with either cetyl alcohol (CA) or HD. This work showed a faster initial rate of polymerization when HD rather than CA was used as a cosurfactant, which resulted in a more narrow particle-size distribution. The polymerization rate–conversion curves of the miniemulsion polymerization with CA revealed a similar profile observed with the conventional emulsion polymerization. Choi et. al.[21] reported the kinetics of S miniemulsion polymerization carried out by using both a water-soluble (potassium persulfate) and an oil-soluble [2,2′-azobis-(2-methyl butyronitrile)] initiator with SLS and CA. They suggested that the polymerization mechanism with the oil-soluble initiator was similar to that observed with the persulfate initiator even though their primary radical generation sites were different. Only the radicals entering from the aqueous phase are capable of propagating radicals in the polymer particles.

In our current experiments, the polymerization rate–conversion curves with and without HD (Figs. 2 and 9) showed a similar polymerization rate profile to that of the miniemulsion polymerization with the hydrophobic additive as a cosurfactant. The mechanism of radical formation from an oil-soluble initiator influences the polymerization kinetics through the distribution of free radicals in the particles and, therefore, through the average number of radicals per particles.[22] In Figure 18, the average number of radicals per particles, $\bar{n}$, obtained from the rate equation given for emulsion polymerization, is plotted against the fractional conversion for the four polymerization systems listed in Table VI. With an HD of content 10.3 mol % as shown in Figure 18(a), $\bar{n}$ decreased with increasing the fractional conversion. In addition, since $\bar{n}$ of the run with $NaNO_2$ is far less than that without $NaNO_2$, it becomes clear that the radicals generated from the water-soluble inhibitor deactivate the free radicals in the particles. On the other hand, in the run without HD as shown in Figure18(b), $\bar{n}$ increased slightly until 0.3 of the fractional conversion and stayed almost constant from 0.3 to 0.55 of the fractional conversion. The influence of a water-soluble inhibitor is less enhanced than is the presence of HD. The particles with HD [Fig. 18(a)] has a larger number of $\bar{n}$ than those without HD regardless of the presence or absence of $NaNO_2$.

For the polymerization with HD, incompatibility between the polymeric radicals and HD plays an essential role for the mechanism. In addition, the termination of radicals by a chain-transfer reaction to HD will be possible to take place as discussed in the previous section. The probability that the desorptions of initiator radicals before reacting with monomer molecules and radicals other than the initiator radicals will occur should be lower than that in the polymerization without HD. In the initial stage of polymerization, the decomposition of the initiator and the subsequent chain growth will take place in the monomer droplets. The homogeneity of the S/HD mixture will be soon lost after the substantial numbers of oligomer radicals were generated because it is a poorer solvent for polystyrene than is the monomer itself [δ_S = 9.6, δ_{HD} = 8.2, and $\delta_{polystyrene}$ = 8.6–9.7 $(cal/cc)^{1/2}$].[23] The oligomeric radicals are apt to precipitate or exist in a coiled conformation, and in either state, the probability of the termination by recombination will decrease. It was proved experimentally that the S oligomers with five units or more are no longer soluble in HD.[24] The accumulation of radicals, well known for precipitation polymerization,[25] takes place in this polymerization with HD. From the simple calculations, $\bar{n}$ divided by the number of initiated radicals per second in a droplet, the average lifetime of radicals is estimated as 15.2 s at the fractional conversion of 0.12, whereas the lifetime decreases to 2.6 s at 0.49 of the conversion. In other words, the longer lifetime of radicals accounts for the high number of $\bar{n}$ in the early stage of polymerization. As the polymerization progresses, the number of polymer chains will progress in parallel. Finally, the phase-separated domains of HD become visible in an optical microscopic scale as shown in Figure 19(b–d). It was observed that the macrodomain of HD appeared on the particle surface at the fractional conversion of 0.33 [Fig. 19(b)]. Notice that this kind of phase separation was not observed in the polymerization without HD as the photographs shown in Figure 19(f) clearly indicated. Therefore, it may be reasonable to assume that the separation of HD from the polystyrene/S phase started from the earlier stage of polymerization, and the polymeric radicals gradually recovered a favorable extended

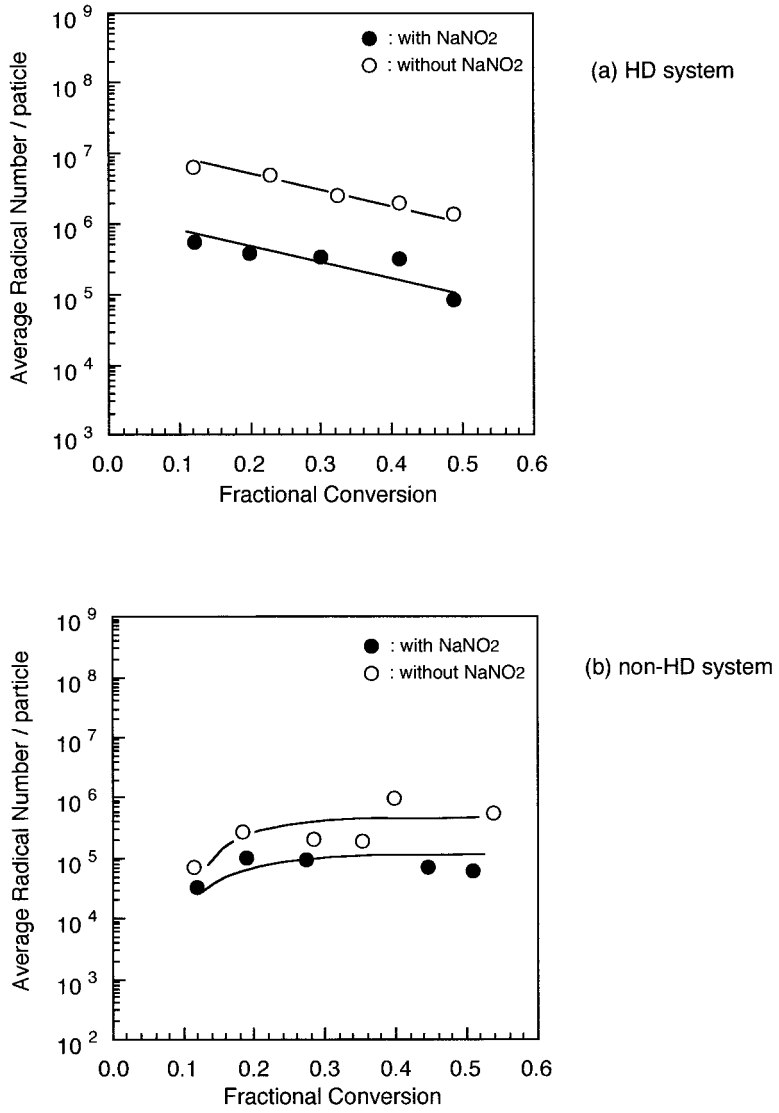

Figure 18 Average particle radical number during polymerization of S droplets: (a) HD = 10.3 mol %; (b) HD = 0.0 mol %. (○) $NaNO_2$ 0.000 mol/L; (●) $NaNO_2$ 0.005 mol/L.

conformation and mobility in the S-rich phase. The termination between two radicals will resume its intensity, leading to the gradual decrease in $\bar{n}$. This trend continues until the viscosity in the droplet increases so high as to obstruct the mobility of the polymer chains and induce the gel effect.

At the earlier stage of the polymerization, it is assumed that the oligomeric radicals are compartmentalized through the process of phase transition from the homogeneous state to the microphase separation states in the particles. This situation in the droplet is sketched in Figure 20 in the Appendix, the droplet being composed of the tiny compartments in which polymeric radicals are isolated (segregated) in the S-rich medium and the surrounding S/HD medium. A stochastic approach may be justified since the number of radicals in the droplet is of the order of 10^6. That the initial polymerization rate was proportional to the 0.24th power of the initiator concentration can be mathematically derived as shown in the Appendix, if the following hypotheses are granted:

1. The volume fraction of the compartments (cells) are small compared to that of the surrounding (continuous) medium;
2. The termination by recombination of radicals is dominated in the continuous medium; and
3. In the cells, the termination between the

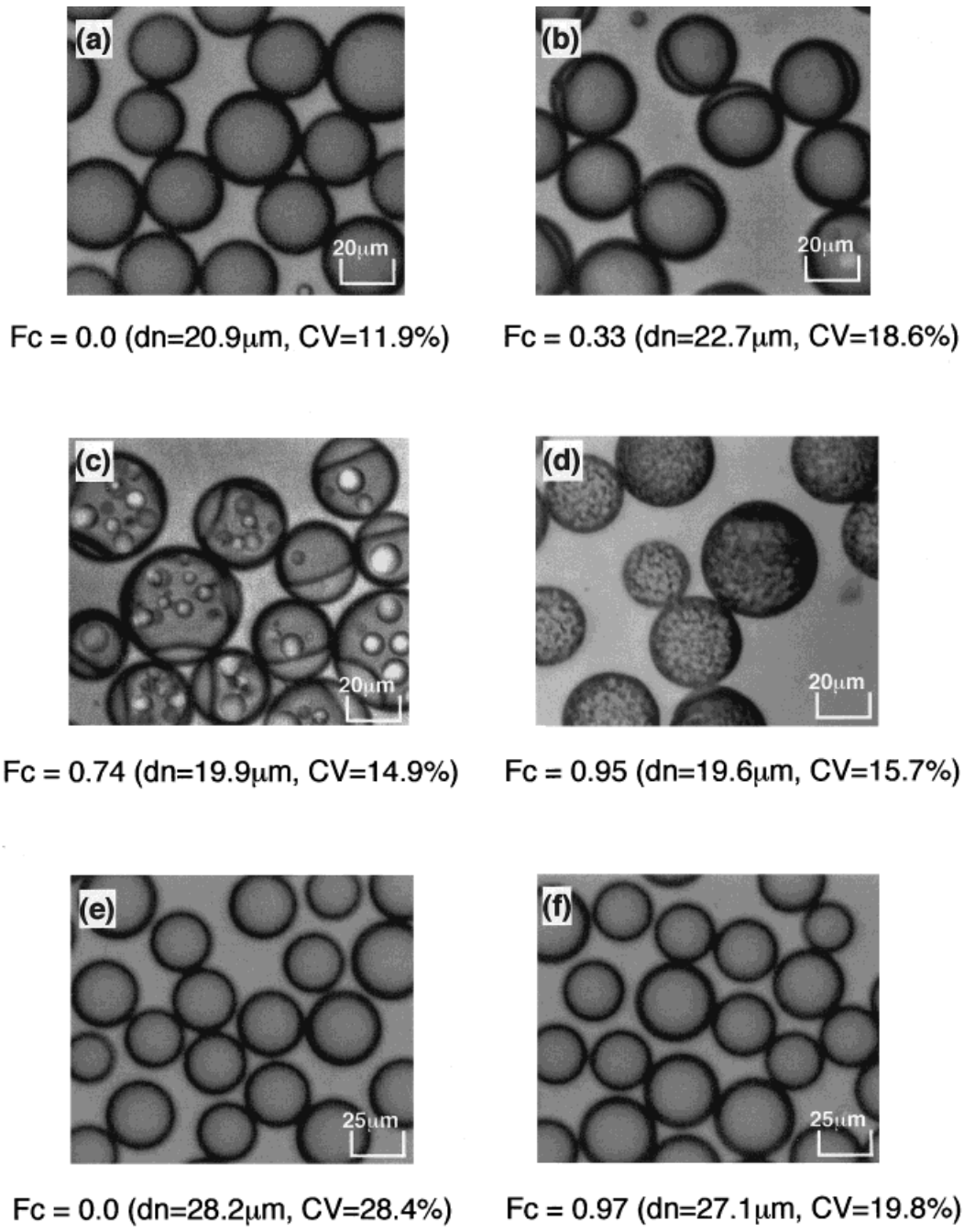

Figure 19 Optical photomicrographs of emulsion during polymerization of S particles (a–d) in the presence of HD and (e,f) in the absence of HD, where *Fc* is the fractional conversion, *dn* = number-average monomer droplet or polymer particle size, and CV is the coefficient of variation: (a) 0% of conversion; (b) 33% of conversion; (c) 74% of conversion; (d) 95% of conversion; (e) 0% of conversion; (f) 97% of conversion.

radicals, mainly polymeric and small radicals, prevails rather than does the desorption of the small radicals into the background medium.

Although we do not have much substantial information for the rate constant (k_i) and the parameters (v_c and N_c, at least, by considering the compartmentalized model, we could speculate about a possible mechanism which resulted in the 0.24th power dependence of the polymerization rate to the initiator concentration As we have shown, the initial polymerization rate, r_{p0}, depends on the number of cells in the particles

which will depend on the amount of HD. It was proved that the r_{p0} for the polymerization with high HD contents was faster than that of the corresponding low HD content: r_{p0} (0 mol % HD) = 1.03×10^{-4} mol L^{-1} s^{-1}, r_{p0},(5.1mol % HD) = 2.69×10^{-4} mol L^{-1} s^{-1} (not shown in the figure), and r_{p0} (10.3 mol % HD) = 3.82×10^{-4} mol L^{-1} s^{-1}; each value was obtained from the droplet prepared with a 2.9-μm SPG pore size. As the polymerization proceeds, HD molecules start to separate from the S/HD medium because of the accumulation of polystyrene chains. Gradually, microdomains of HD are formed, gathering and eventually forming separated macrodomains in the droplets, which are visible by an optical microscope.

On the other hand, in the non-HD system, the hydrophobicity of the droplets was less enhanced than were those of the HD system. The desorption of radicals and the minor generation of radicals by the initiator dissolved in the aqueous phase played a substantial role in the polymerization mechanism of the non-HD system. It can be assumed that the desorption of radicals occurred at the initial stage of polymerization. In addition, the slower polymerization rate up to the fractional conversion of 0.3 (see Fig. 8) implied the entry of inhibiting radicals generated from the water-soluble inhibitor (see Fig. 15). The mechanism of polymerization obeyed that of bulk polymerization because the desorbed radicals were deactivated by the inhibitor in the aqueous phase ($NaNO_2$).

However, when the water-soluble inhibitor was not present, the number of polymer particles increased until 0.3 of the fractional conversion, as shown in Figure 16. Obviously, the desorbing radicals maintained their activity and generated smaller polymer particles by the mechanism of emulsion polymerization. The bimodal particle-size distribution as shown in Figure 17 confirmed the formation of smaller particles. Almog and Levy[26] observed the same result in their suspension polymerization of S with the 10-μm droplet size by employing an oil-soluble initiator and a mixed stabilizer (PVA plus SLS). The initial increase in $\bar{n}$ in Figure 18(b) (without $NaNO_2$) up to the fractional conversion of 0.3 was attributed mainly to the generation of secondary loci rather than to the gradual decrease of entry of the inhibiting radicals (with $NaNO_2$).

CONCLUSIONS

The unique mechanism of suspension polymerization of uniform S droplets was investigated. The homogeneous mixture of S, water-insoluble HD, and BPO was emulsified with the glass membrane (SPG) emulsification technique, forming uniform-sized droplets ranging from 5.6 (1.0-mgr;m pore size) to 20.9 μm (2.9-μm pore size) in average diameter. By the addition of HD, the droplets were stable, without coalescence and breakup during the polymerization. The S/HD mixture was rather incompatible with polystyrene, implying that the polystyrene radicals were isolated in tiny compartments (cells) dissolved in the S-rich medium. These cells were surrounded by the S/HD phase. The initial behavior of polymerization was speculated on by considering a theoretical prediction of $\bar{n}$ (average number of radicals per particle) based on the Smith–Ewart theory (see the Appendix). As the polymerization progressed, the HD phase started to separate from the polystyrene/S phase, and the macrodomain was formed on the surface of the droplets (polymer particles) at the fractional monomer conversion of 33% $\bar{n}$ decreased steadily until increase of the viscosity induced the gel effect. Obviously, the termination by recombination of radicals gradually took over, and the polymerization proceeded in accordance with the homogeneous bulk polymerization mechanism.

In the second series of experiments which were carried out without the addition of HD, no phase transition was observed, and the polymerization behaved as an ordinary suspension polymerization process. Smooth and homogeneous polymer particles were obtained.

As expected, the stability of the monomer droplets was no longer maintained in the runs without the addition of HD in the oil phase and sodium nitrite in the aqueous phase. Some of the initial droplets were wasted as they were consumed by supplying monomers for the growth of secondary particles. These experiments made clear that the water-insoluble substance (HD) and the water-soluble inhibitor (sodium nitrite) were both essential for the preparation of uniform-sized polymer particles by employing the SPG emulsification technique.

APPENDIX: PROPOSED REACTION MECHANISM IN ISOLATED DROPLETS IN THE EARLY STAGE OF POLYMERIZATION

The droplets are composed of an oil-soluble initiator (BPO), S, and HD. We may assume that the all the droplets are isolated because of the low desorption of radicals from them and no entry

from the aqueous phase (regarded as a sink). Suppose that each droplet is compartmentalized in tiny cells (c) as shown in Figure A.1. These cells may dissolve 0, 1, or a few growing radicals in an S-rich environment. These cells are surrounded by the S/HD phase (o), which is by no means a good solvent for polystyrene and the growing radicals.

According to the models proposed by Ugelstad et al.[27] and Kubota et al.[28] based on the Smith–Ewart theory[29] for the kinetics of emulsion polymerization, equations of the radical balance can be written for two phases. Assuming the quasi-steady-state situation for each phase,

$$\alpha_c + y - m_c\bar{n}_c - \bar{n}_c^2 = 0 \tag{A.1}$$

$$\alpha_c + m_c\bar{n}_c - y - \gamma y^2 = 0 \tag{A.2}$$

$$\alpha_c = \frac{r_{ic}v_cN_A}{k_{tc}N_A}, \quad \alpha_0 = \frac{r_{io}v_cN_A}{k_{tc}N_c}, \quad m_c = \frac{k_fv_cN_A}{k_{tc}}$$

$$\gamma = \frac{k_{tc}k_{to}}{k_i^2v_cN_cN_A}, \quad y = \frac{k_iv_cN_A}{k_{tc}N_c}R_o$$

where r_{ic} and r_{io} are the rate of initiation initiated in the cell and the S/HD phase; v_c, the cell volume; N_c, the number of cells in each droplet; $\bar{n}_c$, the average number of radicals in the cell; R_o, the radical concentration in the S/HD phase; and k_{tc} and k_{to}, the rate constants of termination by the recombination of radicals that occurred in the cell and the S/HD phase; k_f, the rate constant of radical desorption from the cell; and k_i, the rate constant of entry of radicals to the cell.

Adding up each side of eq. (A.1) and eq. (A.2), we obtain

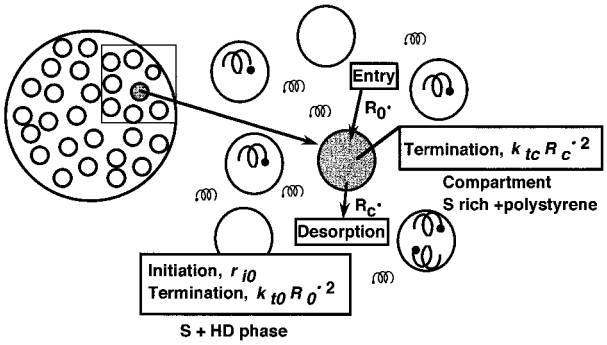

Figure A.1 Schematic representation of isolated droplets in the early stage of polymerization in the presence of HD.

$$\alpha_c + \alpha_o - \bar{n}_c^2 - \gamma y^2 = 0 \tag{A.3}$$

If $\gamma y^2 \gg \bar{n}_c{}^2$ or if the termination is the S/HD phase prevails, then y will be expressed as

$$y = \left(\frac{\alpha_c + \alpha_0}{\gamma}\right)^{1/2} \tag{A.4}$$

In eq. (A.1), if we could further assume that $\bar{n}_c^2 > m_cn_c$, in other words, the radicals inside the cell prefer to terminate each other rather than desire to go into the outer phase, then $\bar{n}_c$ will be expressed as

$$\bar{n}_c = \left[\alpha_c + \left(\frac{\alpha_c + \alpha_0}{\gamma}\right)^{1/2}\right]^{1/2} \tag{A.5}$$

Considering that in the initial stage of the polymerization the polymer concentration is low, then the volume fraction of the total cells will be negligible, and eventually we obtain

$$\bar{n}_c = \left(\frac{\alpha_c + \alpha_0}{\gamma}\right)^{1/4} = \left(\frac{\alpha}{\gamma}\right)^{1/4}$$

$$\alpha = \frac{r_iv_cN_A}{k_{tc}N_c} \tag{A.6}$$

Kubota and Omi[28] derived the same solution of $\bar{n}$ for the extreme case where the termination in the aqueous phase prevails and the desorption of radicals from the polymer particles is low in their attempt to derive approximate solutions of $\bar{n}$ for the precipitation polymerization system.

The rate of polymerization in each droplet can be expressed as

$$r_{p,\text{droplet}} = k_p[M]_oR_o + k_p[M]_c\bar{n}_cN_c \tag{A.7}$$

where $[M]_o$ and $[M]_c$ are the monomer concentration in the S/HD phase and in the cell, respectively. Notice that the dimension of N_c is *mol/L* in this discussion.

Since the HD content is 20 wt % (see Table I), $[M]_o$ and $[M]_c$ will not be so much different. If the polymerization progresses dominantly in the cells, the polymerization rate in the total system will be obtained from eq. (A.7):

$$r_p = r_{p,\text{droplet}}N = k_p[M]_c\bar{n}_cN_cN$$
$$= k_p\left(\frac{r_i}{r_{to}}\right)^{1/4}\left(\frac{k_iv_cN_A}{k_{tc}}\right)^{1/2}[M]_cN_cN \tag{A.8}$$

The dimension of N is L^{-1}. $[M]_o$ may be replaced with the monomer concentration in the droplets; then, finally, we obtain

$$r_p = k_p\left(\frac{r_i}{k_{t0}}\right)^{1/4}\left(\frac{k_i v_c N_A}{k_{tc}}\right)^{1/2}[M]N_c N \qquad \text{(A.9)}$$

Under the fixed volume of the oil phase, v_c (the cell volume) may slightly decrease with increasing initiator concentration, whereas N_c will increase naturally. Compensating for each other, $v_c^{1/2}N_c$ will not be so drastically affected by the change of the initiator concentration. It can be said that the initial rate of polymerization is proportional to 0.25th power of the initiator concentration.

REFERENCES

1. Nakashima, T.; Shimizu, M.; Kukizaki, M. In Membrane Emulsification Operation Manual; Industrial Research Institute of Miyazaki Prefecture: Miyazaki, Japan, 1991.
2. Omi, S.; Katami, K.; Taguchi, T.; Kaneko, K.; Iso, M. Macromol Symp 1995, 92, 309.
3. Omi, S. Colloids Surf A Physicochem Eng Aspects 1996, 97, 109.
4. Omi, S.; Nagai, M.; Ma, G.-H. In 2nd World Congress on Emulsion, Bordeaux, France, 1997; Vol. 4, p 99.
5. Omi, S.; Nagai, M.; Ma, G.-H. Macromol Symp, in press.
6. Yuyama, H.; Watanabe, T.; Ma, G.-H.; Nagai, M.; Omi, S. Colloids Surf A Physicochem Eng Aspects 2000, 168, 159.
7. Karfas, G.; Ray, W. H. Ind Eng Chem Res 1993, 32, 1822.
8. Karfas, G.; Ray, W. H. Ind Eng Chem Res 1993, 32, 1831.
9. Miller, C. M.; Blythe, P. J.; Sudol, E. D.; Silebi, C. A.; El-Aasser, M. S. J Polym Sci Part A Polym Chem Ed 1994, 32, 2365.
10. Miller, C. M.; Sudol, E. D.; Silebi, C. A.; El-Aasser, M. S. J Polym Sci Part A Polym Chem Ed 1995, 33, 1391.
11. Haward, R. N. J Polym Sci 1949, 4, 273.
12. Blackley, D. C. In Emulsion Polymerization; Piirma, I., Ed.; Academic: New York, 1982; Chapter 4.
13. Omi, S.; Katami, K.; Yamamoto, A.; Iso, M. J Appl Polym Sci 1994, 51, 1.
14. Asua, J. M.; Rodriguez, V. S.; Silebi, C. A.; El-Aasser, M. S. Makromol Chem Macromol Symp 1990, 35/36, 59.
15. Alduncin, J. A.; Asua, J. M. Polymer 1994, 35, 3758.
16. Polymer Handbook, 3rd ed.; Brandrup, J.; Immergut, E. H., Eds.; Wiley: New York, 1989.
17. Alduncin, J. A.; Forcada, J.; Asua, J. M. Macromolecules 1994, 27, 2256.
18. Fitch, R. M., personal communication, 1994.
19. Sudol, E. D.; El-Aasser, M. S.; Vanderhoff, J. W. J Polym Sci Polym Chem Ed 1986, 24, 3515.
20. Tang, P. L.; Sudol, E. D.; Silebi, C. A.; El-Aasser, M. S. J Appl Polym Sci 1991, 34, 1059.
21. Choi, Y. T.; El-Aasser, M. S.; Sudol, E. D.; Vanderhoff, J. W. J Polym Sci Polym Chem Ed 1985, 23, 2973.
22. Asua, J. M.; Rodriguez, V. S.; Sudol, E. D.; El-Aasser, M. S. J Polym Sci Part A Polym Chem Ed 1989, 27, 3569.
23. Van Krevelen, D. W.; Hoftyzer, P. J. In Properties of Polymers; Van Krevelen, D. W., Ed.; Elsevier: New York, 1972; Chapter 8.
24. Yuyama, H., unpublished data, 1999.
25. Bamford, C. H.; Bard, W. G.; Jenkins, A. D.; Onyon, D. F. In The Kinetics of Vinyl Polymerization by Radical Mechanisms; Butterworth: London, 1958.
26. Almog, Y.; Levy, M. J Polym Sci Polym Chem Ed 1980, 18, 1.
27. Ugelstad, J.; Mork, P. C.; Hansen, O. A. J Polym Sci Part A-1 1967, 5, 2281.
28. Kubota, H.; Omi, S. J Chem Eng Jpn 1972, 5, 39.
29. Smith, W. V.; Ewart, R. H. J Chem Phys 1948, 16, 592.